

Hartree-Fock-Bogoliubov calculation of charge radii of Sn, Ba, Yb, and Pb isotopes

Shouichi Sakakihara ^{*}, Yasutoshi Tanaka [†]

*Department of Environmental Technology and Urban Planning,
Nagoya Institute of Technology, Gokiso, Nagoya 466-8555, Japan*

Charge radii of Sn, Ba, Yb, and Pb isotopes are calculated within Hartree-Fock-Bogoliubov theory with a Skyrme force and a density-dependent delta-force pairing. We investigate mean field effects of the pairing upon odd-even staggering of isotope shifts. HFB equations are solved in the canonical basis. Odd nuclei are treated in the blocking approximation.

PACS: 21.10.Dr; 21.10.Ft; 21.60.Jz

Keywords: isotope shifts; Hartree-Fock-Bogoliubov theory; Skyrme force; density-dependent pairing

I. INTRODUCTION

Odd-even staggering of isotope shifts is a common phenomena observed in many isotopic chains [1]. The results are interpreted as due to changes in the charge radii of these isotopes, i.e., charge radii of odd-neutron nuclei are smaller than the average radii of their even neighbors [1].

Probable mechanisms so far presented for odd-even staggering of isotope shifts are; core polarization by valence neutrons [2,3], and mean field effects of a three-body (or a density-dependent) pairing force [4–8]. Core polarization effects were first investigated by Talmi [2] as a possible mechanism for producing odd-even staggering of isotope shifts. He could show a remarkably good fitting to changes in the charge radii of Ca isotopes, though it is not certain whether the shell model calculation with a realistic force can reproduce absolute magnitude of isotope shifts. An alternative mechanism was suggested by Zawischa et al. [4–7]. They have demonstrated the importance of a density dependent pairing as well as mean field effects of the pairing on the odd-even staggering of isotope shifts. They could obtain good fitting to changes in the charge radii of Ca, Ba, Sn, and Pb isotopes.

In this paper we investigate in detail the latter possibility employing the HFB theory with axially-symmetric deformation. We assume the Skyrme SLy4 parameterization [11] and the delta-force pairing with linear density dependence [8]. We solve HFB equations in the canonical basis [9,10]. Odd nuclei are treated in the blocking approximation.

This paper is organized as follows. In Section 2, we review some theoretical formalism useful for our purposes. In Section 3, we give numerical results and discussions on Sn, Ba, Yb, and Pb isotopes. Summary and conclusions are given in Section 4.

II. FORMALISM

We follow the HFB scheme prescribed by Reinhard et al [9]. We start with the Hamiltonian,

$$H = T + V^{Skyrme} + V^{pair}, \quad (1)$$

$$V^{pair}(1, 2) = V_0 \frac{1 - \boldsymbol{\sigma}_1 \cdot \boldsymbol{\sigma}_2}{4} \delta(\mathbf{r}_1 - \mathbf{r}_2) \left(1 - \frac{\rho(\frac{\mathbf{r}_1 + \mathbf{r}_2}{2})}{\rho_c} \right). \quad (2)$$

^{*}E-mail shouichi@npl4.kyy.nitech.ac.jp

[†]E-mail tanakay@ks.kyy.nitech.ac.jp

Here V^{Skyrme} is the Skyrme force and V^{pair} is the density-dependent delta-force pairing [8]. The pairing force involves two parameters, i.e., V_0 sets the strength of the force and ρ_c determines its spatial dependence.

The BCS ansatz for the wave function of a pairing many-body system

$$|\Phi_{BCS}\rangle = \prod_{i>0} (u_i + v_i a_i^\dagger a_{\bar{i}}^\dagger) |-\rangle \quad (3)$$

requires that the single particle states are orthonormalized and that occupations add up to the total particle number $\sum v_\alpha^2 = N$. This ansatz carries two key densities [12]. One is the one-body density,

$$\rho_q(\mathbf{r}) = \sum_{\sigma} \langle \Phi_{BCS} | a_{\mathbf{r}\sigma q}^\dagger a_{\mathbf{r}\sigma q} | \Phi_{BCS} \rangle = \sum_i v_i^2 \sum_{\sigma} \phi_i(\mathbf{r}, \sigma, q) \phi_i^*(\mathbf{r}, \sigma, q), \quad (4)$$

and the other is the pairing density,

$$\tilde{\rho}_q(\mathbf{r}) = \sum_{\sigma} (-2\sigma) \langle \Phi_{BCS} | a_{\mathbf{r}-\sigma q} a_{\mathbf{r}\sigma q} | \Phi_{BCS} \rangle = \sum_i u_i v_i \sum_{\sigma} \phi_i(\mathbf{r}, \sigma, q) \phi_i^*(\mathbf{r}, \sigma, q). \quad (5)$$

Here \mathbf{r} , σ , and q denote the space, spin, and charge state of a nucleon, respectively.

We assume the Skyrme force in the particle-hole channel, while the pairing force in the particle-particle channel. Thus the energy separates into a mean-field part and a pairing part as

$$E[\phi, v] = \langle \Phi_{BCS} | H | \Phi_{BCS} \rangle = E_{HF}[\phi, v] + E_{pair}[\phi, v]. \quad (6)$$

E_{HF} is the Skyrme Hartree-Fock energy and E_{pair} is the pairing energy,

$$E_{pair}[\phi, v] = \frac{V_0}{4} \sum_q \int \tilde{\rho}_q^2(\mathbf{r}) \left(1 - \frac{\rho(\mathbf{r})}{\rho_c} \right) d\mathbf{r}. \quad (7)$$

Variation of the energy E with respect to a single-particle wave function is written as

$$\frac{\delta E}{\delta \phi_i^*} = \hat{\mathcal{H}}_i \phi_i, \quad (8)$$

$$\hat{\mathcal{H}}_i = v_i^2 (\hat{h}_{Skyrme} + \Gamma_{pair}(\mathbf{r})) + u_i v_i \Delta_q(\mathbf{r}). \quad (9)$$

Variation of E_{HF} yields the Skyrme Hartree-Fock hamiltonian \hat{h}_{Skyrme} , while variation of E_{pair} yields the pair mean-field Γ_{pair} as well as the gap potential Δ_q . The pair mean-field Γ_{pair} comes from the variation of the density $\rho_q(\mathbf{r})$ in Eq. (7). It has the form

$$\Gamma_{pair}(\mathbf{r}) = -\frac{V_0}{4\rho_c} (\tilde{\rho}_n^2(\mathbf{r}) + \tilde{\rho}_p^2(\mathbf{r})). \quad (10)$$

The gap potential Δ_q comes from the variation of the pairing density $\tilde{\rho}_q(\mathbf{r})$ in Eq. (7). It has the form

$$\Delta_q(\mathbf{r}) = \frac{V_0}{2} \tilde{\rho}_q(\mathbf{r}) \left(1 - \frac{\rho(\mathbf{r})}{\rho_c} \right). \quad (11)$$

It is noted that the pair mean-field Γ_{pair} does not depend on the charge state. It is always repulsive and arises only from the density dependent pairing. On the other hand, the gap potential Δ_q depends on the charge state q and arises from any pairing force irrespective of its density dependence. For a density parameter ρ_c lower than the central density, the gap potential will be repulsive inside the nucleus and it is attractive at the nuclear surface.

A single particle hamiltonian \mathcal{H}_i of Eq. (9) depends on the state i . It is not hermitian in contrast to HF + BCS calculations. Therefore variation actually needs to take care of the orthonormality of the wave functions as

$$\frac{\delta}{\delta\phi_i^*} \left(E - \sum_{ij} \Lambda_{ij} \left(\int \phi_j^*(\xi) \phi_i(\xi) d\xi - \delta_{ij} \right) \right) = 0, \quad (12)$$

where ξ represents all variables. The equation leads to a generalized mean-field equation,

$$\hat{\mathcal{H}}_i \phi_i = \sum_j \Lambda_{ji} \phi_j. \quad (13)$$

Lagrange multipliers Λ_{ij} constitute a symmetric matrix $\Lambda_{ij} = \Lambda_{ji}$.

Variation of the energy with respect to the occupation probability under the particle number constraint yields

$$\frac{d}{dv_i} \left(E - \lambda \sum_j v_j^2 \right) = 2v_i h_{ii} + (\Delta_{ii})_q \left(\frac{v_i^2}{u_i} - u_i \right) = 0, \quad (14)$$

$$h_{ii} = \langle \phi_i | \hat{h}_{Skyrme} + \Gamma_{pair}(\mathbf{r}) - \lambda | \phi_i \rangle, \quad (15)$$

and the pairing gap is calculated as

$$(\Delta_{ii})_q = - \int \sum_{\sigma} |\phi_i(\mathbf{r}, \sigma, q)|^2 \Delta_q(\mathbf{r}) d\mathbf{r}. \quad (16)$$

Eq. (14) can be solved in the standard manner and yields

$$\begin{Bmatrix} v_i \\ u_i \end{Bmatrix} = \sqrt{\frac{1}{2} \mp \frac{1}{2} \frac{h_{ii} - \lambda}{\sqrt{(h_{ii} - \lambda)^2 + \Delta_{ii}^2}}}. \quad (17)$$

Both Eqs. (13) and (14) constitute the HFB equation. Eqs. (13) and (14) are solved iteratively employing the gradient method,

$$|\phi_i^{n+1}\rangle = \mathcal{O}\{|\phi_i^n\rangle - \mathcal{D}(\hat{\mathcal{H}}_i^n |\phi_i^n\rangle - \sum_j \Lambda_{ji} |\phi_j^n\rangle)\}. \quad (18)$$

The parameter \mathcal{D} determines the size of the step and \mathcal{O} means Gram-Schmidt orthonormalization. $|\phi_i^n\rangle$ and $\hat{\mathcal{H}}_i^n$ represent a single particle state and the mean field in the n-th iteration, respectively. Lagrange multipliers Λ_{ij} are determined by the orthonormality of the states. They are

$$\Lambda_{ij} = \frac{1}{2} \langle \phi_i^n | \hat{\mathcal{H}}_i^n + \hat{\mathcal{H}}_j^n | \phi_j^n \rangle. \quad (19)$$

III. RESULTS AND DISCUSSIONS

We have investigated changes in the charge radii of Sn, Pb, Ba, and Yb isotopes because long isotopic chains are observed in these nuclei and because they lie in the spherical, transitional and well deformed regions of the nuclear chart, respectively. The parametrization SLy4 [11] is employed for the Skyrme force. The parameters were specifically devised to reproduce correct incompressibility modulus for the symmetric nuclear matter and to improve the isospin property of the force away from the β -stability line.

These features of the SLy4 force are especially favorable to the calculation of charge radii along a long isotopic chain. However, the SLy4 parameters were determined without the pairing correlation and therefore they would have to be modified when they are used in HFB calculations. With the pairing parameters discussed in the next paragraph, it turns out that pair mean-fields Γ_{pair} contribute to HF + BCS results of Sn, Pb, Ba, and Yb isotopes by an order of ten keV and the gap potentials Δ by an order of hundred keV. Gap potentials have non-negligible effects on the odd-even mass difference of isotopes.

However, the effects may be included in the pairing by adjusting its parameters and therefore we assume the original SLy4 parametrization in the following analysis.

The depth and the density parameters of the pairing force are taken as $V_0 = -1250 \text{ MeV}\cdot\text{fm}^3$ and $\rho_c = 0.140 \text{ fm}^{-3}$, respectively. They were obtained by fitting to one-neutron separation energies as well as odd-even staggering of charge radii of the above isotopes. We assumed the same set of pairing parameters for all isotopes. With a fixed value of ρ_c , we determined the depth V_0 by fitting to one-neutron separation energies. We repeated this process for several different values of ρ_c and found the best value of ρ_c by comparing odd-even staggarings of charge radii. With this procedure we obtained a lower density parameter $\rho_c = 0.140 \text{ fm}^{-3}$ than the saturation density $\rho_c = 0.160 \text{ fm}^{-3}$.

In practice, calculated charge-radii also depend on the active pairing space. In the present paper, we take into account all bound levels with energies lower than $e_F + 1\hbar\omega$, where e_F is the Fermi energy and $1\hbar\omega = 41A^{-1/3} \text{ MeV}$. With this prescription, however, we have encountered a problem of convergence. In each step of iterations, some of the highest levels go in and out from the active pairing space, which give rise to an oscillation of the binding energy. Thus for the first few hundred iterations, we excluded the gap potential Δ_q from the mean field hamiltonian and solved the equation by diagonalization. After having had a pretty good convergence, we fixed the number of single-particle levels of the active pairing space and solved the full mean-field equation by employing the gradient step.

We have also studied the cut-off prescription of Bonche et al. [13]. With their prescription, however, we could not reproduce odd-even staggering in light Ba isotopes if we included the positive energy levels in the active pairing space. Except for this difficulty, our cut-off prescription gives similar results to those of Bonche et al. [13].

We assumed $\mathcal{D} = 1/(E_{kin} + 50) \text{ MeV}^{-1}$ as a size of the gradient step. The parameter \mathcal{D} varies during the iterations and E_{kin} is the kinetic energy of the previous iteration. We have also assumed that the iteration has converged if $|\Delta E| < 10^{-4} \text{ MeV}$ for the energy and $|\Delta r| < 10^{-4} \text{ fm}$ for the charge radius between two successive iterations. (We did not have a good solution for ^{125}Sn , where the charge radius fulfilled $|\Delta r| < 10^{-4} \text{ fm}$, but the binding energy oscillated with amplitude of $|\Delta E| \simeq 2 \times 10^{-3} \text{ MeV}$.)

Single particle states were expanded in an deformed oscillator basis with axially-symmetry [14]. Eleven major shells were assumed in the calculation. Eleven major shells are not enough to produce correct binding energies of heavy nuclei. However, by comparing the present results with those of fifteen major shells, we have found that neutron separation energies and isotopic shifts were little affected by the size of the basis space. Odd neutron nuclei were treated in the blocking approximation [15]. Odd neutron contributes to the density ρ , but it does not contribute to the pairing density $\tilde{\rho}$.

Fig. 1 shows calculated results of Sn isotopes along with experiment; (a) neutron separation energies, (b) isotopic shifts in the charge radii of Sn isotopes normalized to the nucleus ^{120}Sn ($\Delta r_c^2 = r_c^2(A) - r_c^2(120)$), and (c) isotopic shifts in the charge radii of Sn isotopes. Experiment is denoted by open circles, while calculation is denoted by crosses. As a guide for eyes, they are connected with solid lines and dashed lines, respectively. We also modified changes in the charge radii of Fig. 1(b) by subtracting an equivalent of the liquid-drop difference, $r_{LD}^2(A) = 3/5r_0^2A^{2/3}$ and $r_0 = 1.2 \text{ fm}$.

Figs. 1(a) and 1(b) show good agreement with experiment both for neutron separation energies and changes in the charge radii of Sn isotopes. Close examination of Fig. 1(b) reveals that charge radii of odd neutron nuclei are smaller than the average radii of their even neighbors. This is a well-known phenomena of odd-even staggering of isotope shifts. In Fig. 1(c) the phenomena is more clearly exhibited by taking the difference of charge radii between neighboring isotopes.

Odd-even staggering of isotope shifts has been a longstanding problem in nuclear physics. Only recently it is realized [4–8] that a density dependence seems to be necessary for the pairing and that mean field effects of the pairing seems to be responsible for this phenomena. Indeed, we cannot predict odd-even staggering of charge radii within a framework of ordinary HF + BCS theory, even if we employ the density dependent pairing in the calculation. We need to take into account mean fields of the pairing to explain the phenomena.

Fig. 2(a) shows the HF + BCS calculation without mean fields of the pairing. As is mentioned above, we could not reproduce odd-even staggering of isotope shifts even if we employed the density dependent pairing in the calculation. Fig. 2(b) shows the HF + BCS calculation with the pair mean-field Γ_{pair} but without the neutron gap-potential Δ_n . Odd-even staggering is now well reproduced except for heavy Sn isotopes. Fig. 2(c) shows the HFB calculation with the gap potential but without the pair mean-field. The figure shows that the gap potential is also responsible for the odd-even staggering. The potential works especially well for heavy Sn isotopes. Reminding that Fig. 1(c) is the full HFB calculation where the pair mean-field and the gap potential are both included in the hamiltonian, we may conclude that the

pair mean-field as well as the gap potential are both responsible for the occurrence of odd-even staggering of Sn isotopes.

Fig. 2(d) shows the pair mean-fields of ^{109}Sn , ^{110}Sn , and ^{111}Sn . Fig. 2(e) shows the neutron gap potentials of the same nuclei. In these figures we show monopole radial shapes of the potentials in the Legendre expansion. From Fig. 2(d) we see that the pair mean-field is repulsive inside a nucleus. The repulsive potential causes a shallow HF field and thus the nucleus expands. Since an even nucleus has a stronger pair mean-field than its odd neighbors, the charge radius of the even nucleus expands more than its odd neighbors. The same is true for the gap potential. Fig. 2(e) shows that the gap potential is repulsive inside a nucleus while it is attractive at the nuclear surface. The potential too, expands the nucleus. The potential is also stronger for an even nucleus than its odd neighbors, leading to a larger charge radius for the even nucleus than its odd neighbors.

It is noted that the pair mean-field has a larger effect than the gap potential on the odd-even staggering of isotope shifts. This is because that the pair mean-field Γ_{pair} exists in the proton HF field even for proton closed-shell nuclei. On the other hand, the proton gap-potential Δ_p vanishes for the proton closed-shell nuclei. For such nuclei, the neutron gap-potential Δ_n affects only indirectly the charge radii of isotopes via the HF fields.

Fig. 3(a) shows one-neutron separation energies of Pb isotopes. Fig. 3(b) shows isotopic shifts in the charge radii of Pb isotopes normalized to the nucleus ^{208}Pb . Fig. 3(c) shows isotopic shifts in the charge radii of Pb isotopes. Good agreement with experiment was obtained both for neutron separation energies and isotopic shifts.

Pb isotopes are similar to Sn isotopes in that the proton shell is closed. However, in contrast to Sn isotopes, the isotopic chain of Pb extends beyond the neutron shell closure at $N=126$. At the shell closure we see in Fig. 3(b) an abrupt change of charge-radius differences, which is called a “kink”.

We have also investigated mean field effects of the pairing on the kink of Pb isotopes. Mean fields of the pairing get stronger as an isotope goes away from ^{208}Pb and strong mean fields could give rise to a larger charge radius. If this is the case, changes in the charge radii of Pb isotopes would be small for nuclei lighter than ^{208}Pb , while they would be large for nuclei heavier than ^{208}Pb . Fig. 3(b) shows isotopic shifts of Pb nuclei from our calculation, the relativistic mean field (RMF) theory [20], and experiment. Our calculation could not predict large enough isotope shifts for nuclei beyond ^{208}Pb . Indeed our calculation is very similar to the HF + BCS calculation without the mean field effects of the pairing. Mean fields of the pairing seem to have only marginal effects on the occurrence of the kink around ^{208}Pb .

The kink around ^{208}Pb may be primarily due to the shell structures in this region of nuclei. The $2g_{9/2}$ neutron level lying close to the continuum seems to be the key to the occurrence of the kink. Indeed the kink is well reproduced with the RMF calculation [20]. The kink is also reproduced with a nonrelativistic Skyrme calculation by omitting the Fock term of the spin-orbit interaction [21] or by assuming the isospin dependence in the spin-orbit energy functional [21,22].

We have so far studied mean field effects of the pairing on the charge radii of spherical nuclei. In the following we will examine mean field effects of the pairing on the charge radii of transitional and well deformed nuclei.

Fig. 4(a) shows neutron separation energies of Ba isotopes. Fig. 4(b) shows isotopic shifts in the charge radii of Ba isotopes. As in the case of Pb isotopes, the isotopic chain extends beyond the shell closure at $N = 82$ and exhibits a kink around ^{138}Ba . Fig. 4(c) shows odd-even staggering of Ba isotopes. Agreement with experiment is in general good.

The kink in Ba isotopes may be due to changes in the nuclear deformation. Proton shells of Ba nuclei are not closed and therefore most Ba nuclei are soft against nuclear deformation. Fig. 4(d) shows calculated quadrupole moments which agree well with experiment [23]. As seen from this figure, the deformation decreases as the neutron number increases toward ^{138}Ba and then the deformation increases beyond ^{138}Ba . Thus changes in the charge radii are small for nuclei lighter than ^{138}Ba , while they are large for nuclei heavier than ^{138}Ba . We see in Fig. 4(b) that our calculation reproduces the kink fairly well, though the deviation from experiment becomes appreciable in the region of light Ba isotopes.

At this point we wish to mention the reason why we have employed a small density parameter $\rho_c = 0.140 \text{ fm}^{-3}$ for the pairing instead of the saturation density $\rho_c = 0.160 \text{ fm}^{-3}$. Fig. 5(a) shows neutron separation energies of Ba isotopes calculated with $\rho_c = 0.160 \text{ fm}^{-3}$ and $V_0 = -1000 \text{ MeV}\cdot\text{fm}^3$. (A strength of $V_0 = -1000 \text{ MeV}\cdot\text{fm}^3$ is necessary in order to fit to neutron separation energies.) Fig. 5(b) shows isotopic shifts between neighboring isotopes calculated with the same set of parameters. By comparing Fig. 4(c) and Fig. 5(b), we see that with this set of parameters odd-even staggering of isotope shifts does not agree well with experiment. Although we have shown Ba isotopes as an example, we have obtained

good results also for Sn and Pb isotopes with $\rho_c = 0.140 \text{ fm}^{-3}$ and $V_0 = -1250 \text{ MeV}\cdot\text{fm}^3$.

In Fig. 6, we show neutron separation energies of Yb isotopes. Agreement with experiment is good. Figs. 6(b) and 6(c) show changes in the charge radii of Yb isotopes. In this case, however, agreement with experiment is rather poor especially for nuclei lighter than ^{165}Yb . Our calculation suggests that odd-even staggering in the charge radii of Yb isotopes might be related to the odd-even staggering of nuclear deformation of these nuclei. For nuclei lighter than ^{165}Yb , a larger deformation is calculated for an even isotope than its odd neighbors. The difference is enough to explain the odd-even staggering of charge radii of these nuclei. For nuclei heavier than ^{165}Yb , however, a larger deformation is calculated for an odd nucleus than its even neighbors. Mean fields of the pairing and nuclear deformation have opposite effects on the charge radii, leading to a rather complicated behavior of isotopic shifts in this region of nuclei.

IV. SUMMARY AND CONCLUSION

We have investigated mean field effects of the pairing on the charge radii of Sn, Pb, Ba, and Yb isotopes. There are two mean fields arising from the pairing energy functional. One is the pair mean-field Γ_{pair} which comes from the density dependent part of the pairing. The pair mean-field does not depend on the charge state and therefore the same form of the pair mean-field appears in the HF fields of protons and neutrons. In addition, the potential exists even for proton closed-shell nuclei. The other is the gap potential which arises from the variation of the pairing density in the pairing energy functional. Therefore the gap potential arises also from the density independent pairing. In contrast to the pair mean field, however, the proton gap potential vanishes for proton closed-shell nuclei.

For the pairing we have employed in the present calculations, the pair mean-field is repulsive inside a nucleus. The repulsive potential causes a shallow HF field and the nucleus expands. Since an even nucleus has a stronger pair mean-field than its odd neighbors, the charge radius of an even nucleus expands more than its odd neighbors. The same is true for the gap potential. It is repulsive inside a nucleus and attractive at the nuclear surface. The potential too, expands the nucleus. Like the pair mean field, the gap potential is stronger for an even nucleus than its odd neighbors. These facts seem to be the key ingredient in the occurrence of odd-even staggering of isotopic shifts.

The present analyses have shown that the lower density parameter $\rho_c=0.140 \text{ fm}^{-3}$ than the saturation density $\rho_c=0.160 \text{ fm}^{-3}$ gives better agreement with experiment in fitting to the odd-even staggering of isotope shifts of Sn, Pb, Ba, and Yb. We have also shown that the kink observed in the charge radii of Ba isotopes may be due to changes in the nuclear deformation. The effects are enough to explain the kink around ^{138}Ba .

ACKNOWLEDGMENTS

We would like to express our sincere appreciation to Ken-ichiro Arita for many fruitful and critical discussions. We would like to thank M. Yamagami and K. Matsuyanagi, and also members of Nagoya Nuclear-Structure Seminar for many illuminating discussions.

-
- [1] P. Aufmuth, K. Heilig, and A. Steudel, *At. Data Nucl. Data Tables* 37 (1987) 455.
 - [2] I. Talmi, *Nucl. Phys. A* 423 (1984) 189.
 - [3] H. Sagawa, A. Arima, and O. Scholten, *Nucl. Phys. A* 474 (1987) 155.
 - [4] U. Regge and D. Zawischa, *Phys. Rev. Lett.* 61 (1988) 149.
 - [5] S. A. Fayans, S. V. Tolokonnikov, E. L. Trykov, and D. Zawischa, *Phys. Lett. B* 338 (1994) 1.
 - [6] E. Krömer, S. V. Tolokonnikov, S. A. Fayans, and D. Zawischa, *Phys. Lett. B* 363 (1995) 12.
 - [7] S. A. Fayans and D. Zawischa, *Phys. Lett. B* 383 (1996) 19.
 - [8] N. Tajima, P. Bonche, H. Flocard, P.-H. Heenen, and M. S. Weiss, *Nucl. Phys. A* 551 (1993) 434.
 - [9] P.-G. Reinhard, M. Bender, K. Rutz, and J. A. Maruhn, *Z. Phys. A* 358 (1997) 277.

- [10] N.Tajima, XVII RCNP International Symposium on Innovative Computational Methods in Nuclear Many-Body Problems, H. Horiuchi *et al.* eds. (World Scientific, Singapore, 1998) p. 343.
- [11] E. Chabanat, P. Bonche, P. Haensel, J. Meyer, and R. Schaeffer, Nucl. Phys. A 635 (1998) 231.
- [12] J. Dobaczewski, H. Flocard, J. Treiner, Nucl. Phys. A 422 (1984) 103.
- [13] P. Bonche, H. Flocard, P. H. Heenen, S. J. Krieger, and M. S. Weiss, Nucl. Phys. A 443 (1983) 39.
- [14] D. Vautherin, Phys. Rev. C 7 (1973) 296; Program “*harfe*”, unpublished.
- [15] P. Ring and P. Schuck, The Nuclear Many-Body Problem (Springer-Verlag, 1980) p. 237.
- [16] G. Audi and A. H. Wapstra, Nucl. Phys. A 595 (1995) 409.
- [17] J. Eberz, U. Dinger, G. Huber, H. Lochmann, R. Menges, G. Ulm, R. Kirchner, O. Klepper, T. U. Kühl, and D. Marx, Z. Phys. A 326 (1987) 121.
- [18] U. Dinger, J. Eberz, G. Huber, R. Menges, S. Schröder, R. Kirchner, O. Klepper, T. Kühl, D. Marx, and G. D. Sprouse, Z. Phys. A 328 (1987) 253.
- [19] S. B. Dutta, R. Kirchner, O. Klepper, T. U. Kühl, D. Marx, G. D. Sprouse, R. Menges, U. Dinger, G. Huber, and S. Schröder, Z. Phys. A 341 (1991) 39.
- [20] M. M. Sharma, G. A. Lalazissis and P. Ring, Phys. Lett. B 317 (1993) 9.
- [21] M. M. Sharma, G. Lalazissis, J. König and P. Ring, Phys. Rev. Lett. 74 (1995) 3744.
- [22] P.-G. Reinhard and H. Flocard, Nucl. Phys. A 584 (1995) 467.
- [23] S. Raman, C. H. Malarkey, W. T. Milner, C. W. Nestor, Jr., and P. H. Stelson, At. Data Nucl. Data Tables 36 (1987) 1.

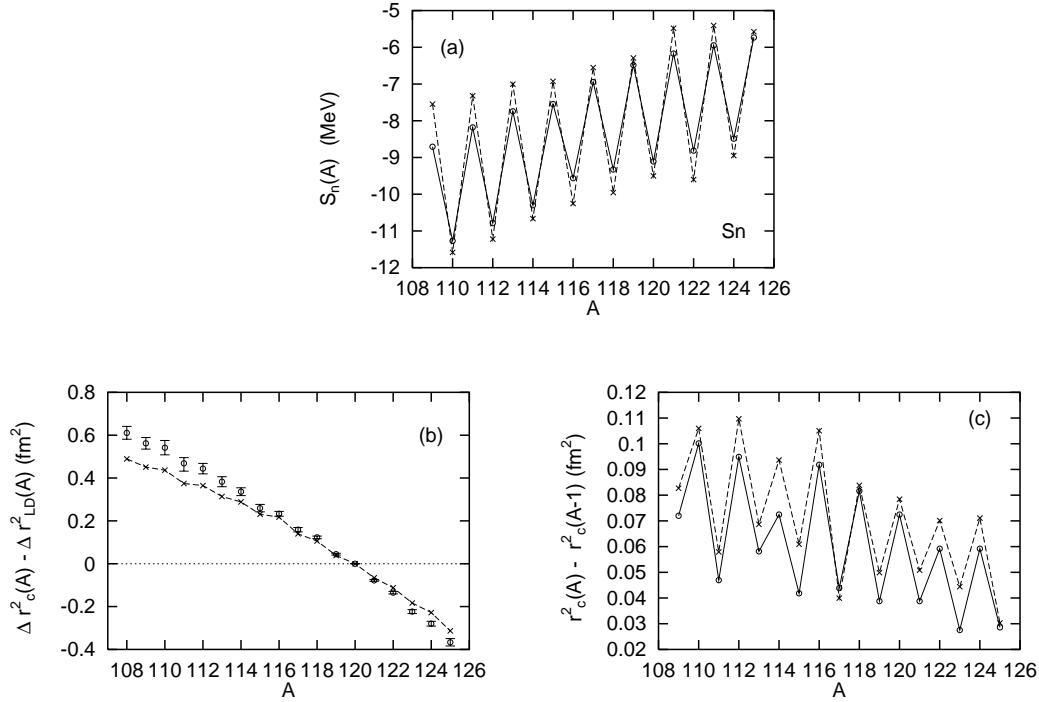


FIG. 1. (a) Neutron separation energies of Sn isotopes. (b) Isotopic shifts in the charge radii of Sn isotopes normalized to the nucleus ^{120}Sn . They are subtracted by an equivalent of the liquid-drop difference. (c) Isotopic shifts in the charge radii of Sn isotopes. Experiment is denoted by open circles, while calculation is denoted by crosses. As a guide for eyes, they are connected with solid lines and dashed lines, respectively. Experimental data are taken from Refs. [1,16,17].

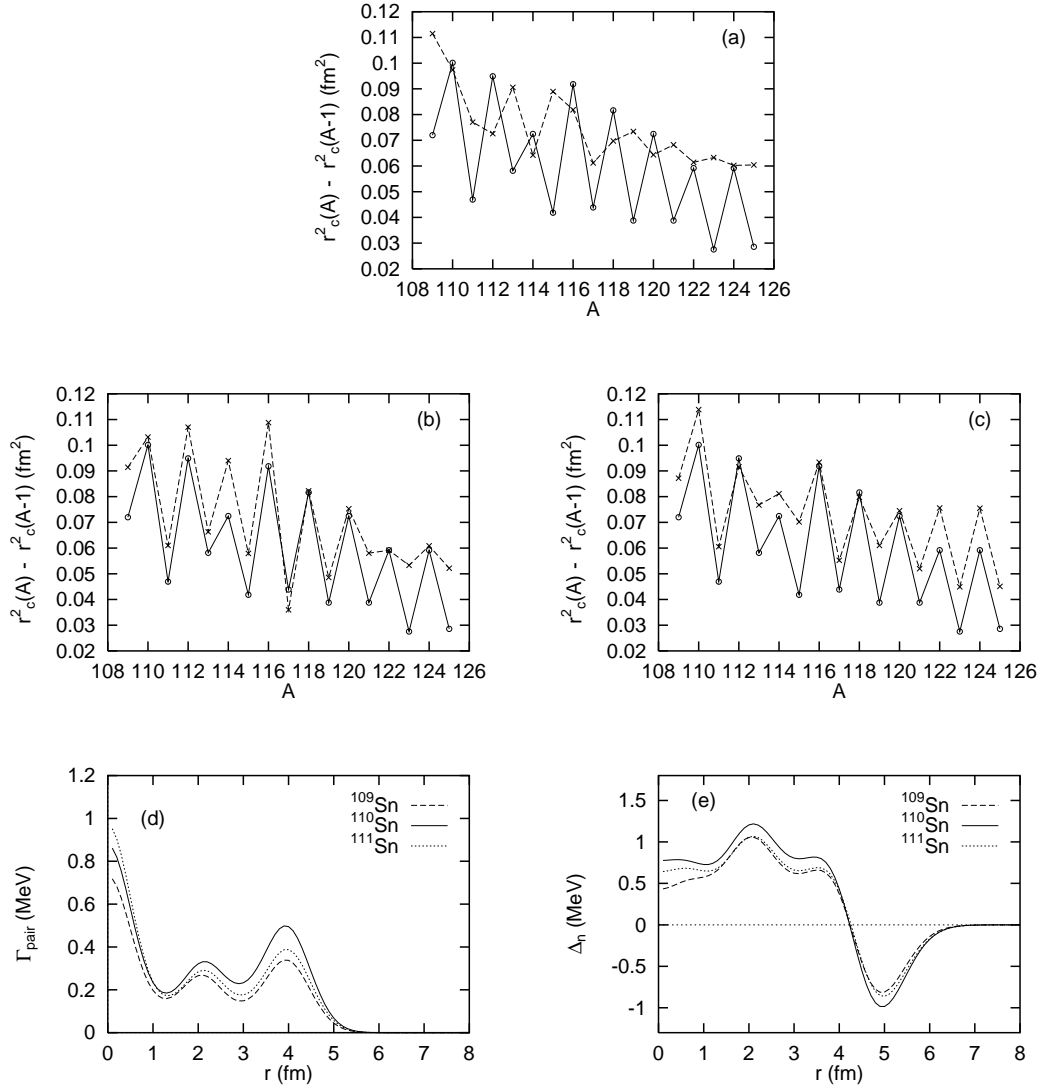
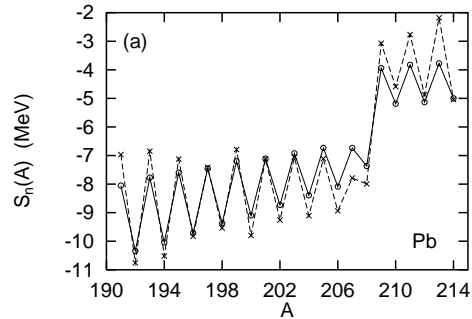


FIG. 2. Mean field effects of the pairing on the isotopic shifts of Sn. (a) The HF+BCS calculation without the mean fields of the pairing. (b) The HF+BCS calculation with the pair mean-field Γ_{pair} but without the neutron gap-potential Δ_n . (c) The HFB calculation with the neutron gap potential but without the pair mean-field. Experiment is denoted by open circles, while calculations are denoted by crosses. (d) Monopole radial shapes of the pair mean-fields. (e) Monopole radial shapes of the neutron gap potentials.



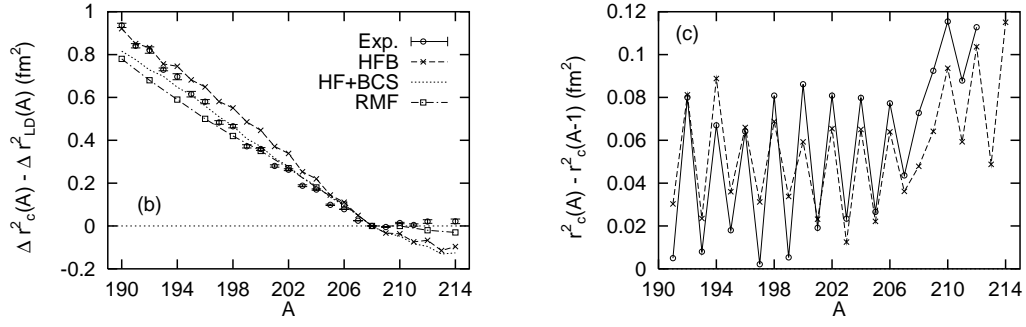


FIG. 3. (a) Neutron separation energies of Pb isotopes. (b) Isotopic shifts in the charge radii of Pb isotopes normalized to the nucleus ^{208}Pb . The RMF calculation of Sharma et al. [20] and the HF + BCS calculation are also shown for comparison. (c) Isotopic shifts in the charge radii of Pb isotopes. Experiment is denoted by open circles, while calculation is denoted by crosses. Experimental data are taken from Refs. [1,16,18,19].

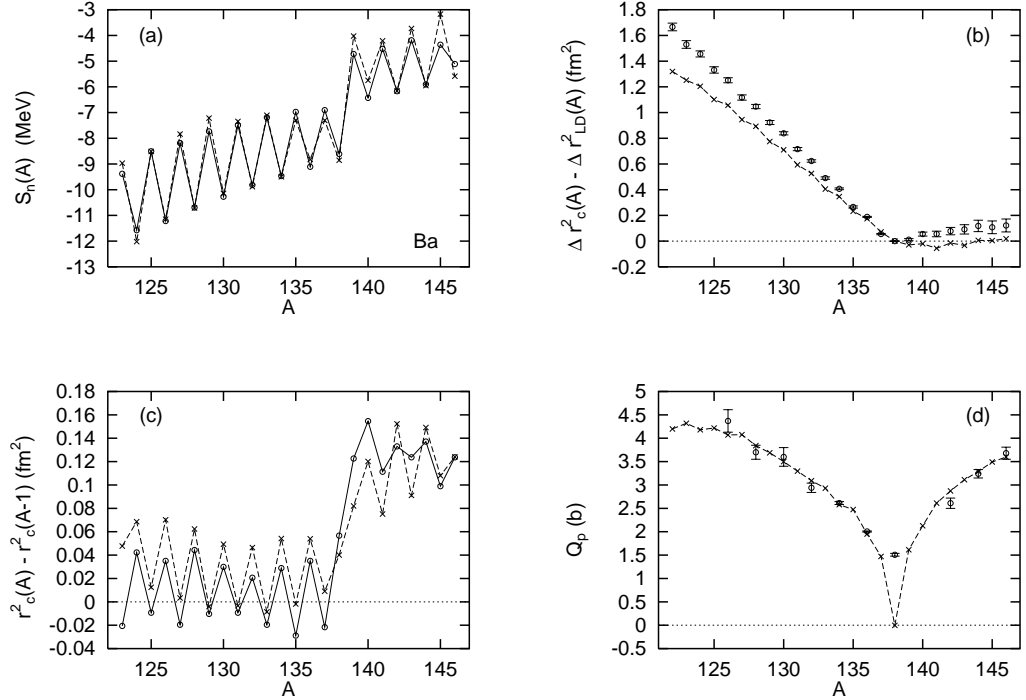


FIG. 4. (a) Neutron separation energies of Ba isotopes. (b) Isotopic shifts in the charge radii of Ba isotopes normalized to the nucleus ^{138}Ba . (c) Isotopic shifts in the charge radii of Ba isotopes. (d) Intrinsic quadrupole moments of Ba isotopes. Experiment is denoted by open circles, while calculation is denoted by crosses. Experimental data are taken from Refs. [1,16,23].

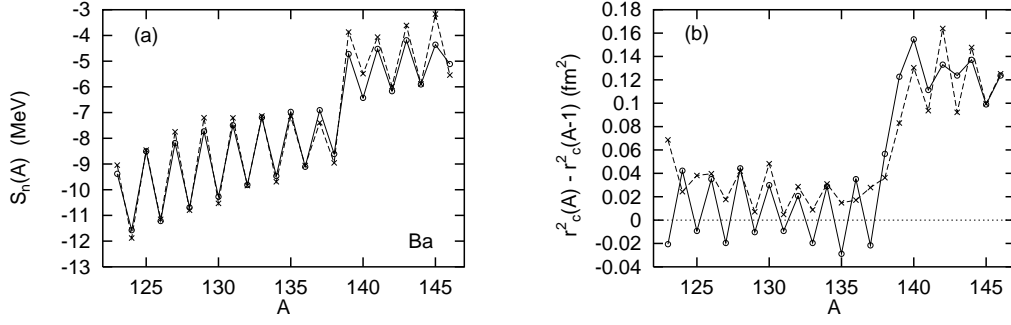


FIG. 5. (a) Neutron separation energies of Ba isotopes calculated with the pairing parameters of $\rho_c=0.160 \text{ fm}^{-3}$ and $V_0 = -1000 \text{ MeV}\cdot\text{fm}^3$. (b) Isotopic shifts in the charge radii of Ba isotopes calculated with the same set of pairing parameters. Experimental data are taken from Refs. [1,16].

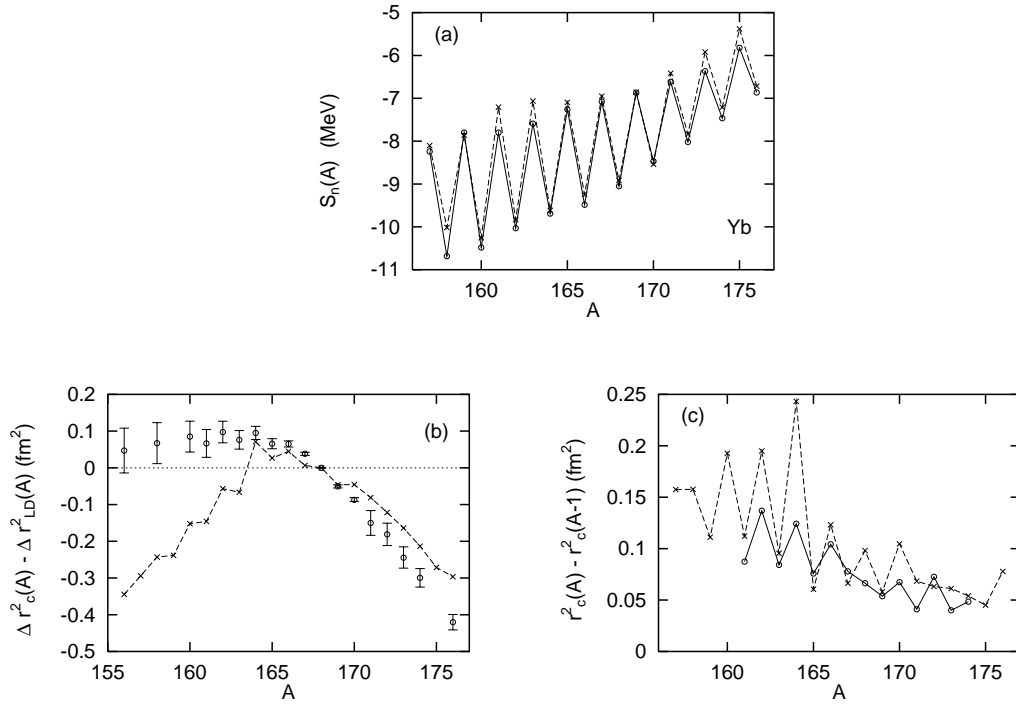


FIG. 6. (a) Neutron separation energies of Yb isotopes. (b) Isotopic shifts in the charge radii of Yb isotopes normalized to the nucleus ^{168}Yb . (c) Isotopic shifts in the charge radii of Yb isotopes. Experiment is denoted by open circles, while calculation is denoted by crosses. Experimental data are taken from Refs. [1,16].